ISSN: 0975-8585

Research Journal of Pharmaceutical, Biological and Chemical Sciences

Effect of ZNO Nanoparticles Dispersed in Liquid Crystalline Alkoxy Benzoic Acids and Periodic Noise Reduction Using Frequency Domain Filtering.

RKNR Manepalli[1]*, P Jayaprada[1], MC Rao[2], BTP Madhav[3], and K Pandian[4].

[1]Department of Physics, The Hindu College, Krishna University, Machilipatnam-521001, India.
[2]Department of Physics, Andhra Loyola College, Vijayawada-520008, India
[3]LCRC-R&D, Department of ECE, K L University, Guntur-522502, India
[4]Department of Inorganic Chemistry, University of Madras, Guindy Campus, Chennai-600025, India

ABSTRACT

In the present work, the synthesis and characterization are carried-out on p-n-Alkoxy benzoic acids namely p-n-Octyloxy benzoic acid (8OBA) and p-n-do decyloxy benzoic acid (12OBA) compounds with 0.5 wt % ZnO nanoparticle dispersion. The Differential Scanning Calorimetry (DSC) technique is used to measure the phase transition temperatures. Further characterization is carried-out by various spectroscopic techniques like UV-visible Spectroscopy (UV), Scanning Electron Microscopy (SEM) and Fourier Transform Infra Red Spectroscopy (FTIR). Textural determinations of the synthesized compounds were recorded by using Polarizing Optical Microscope (POM) connected with hot stage and camera. The results showed that the dispersion of ZnO nanoparticles in 8OBA and 12OBA exhibited NC phases as same as the pure compounds with reduced clearing temperature as expected. Further, the nematic thermal ranges are also increased while performing both DSC and POM with the dispersion of ZnO nanoparticles. Image enhancement is also carried-out to improve the quality of the contrast in the images collected from POM.

Keywords: Synthesis, POM, DSC, Nano dispersion, UV Spectroscopy, SEM, FTIR and Image Enhancement.

Corresponding author

ISSN: 0975-8585

INTRODUCTION

Liquid crystals (LCs) are self-assembled functional soft materials which possess both order and mobility at molecular, supra-molecular and macroscopic levels [1-3]. LCs received much attention in the recent years because of their ability to transfer their long range orientational order on the dispersed materials such as nanoparticles and different colloids [4-10]. Introduction of nanoparticles do not induce significant distortion of LC phases. Nanoscience and nanotechnology are vital frontiers in scientific research. A broad area of research topics from fundamental, physical, biological and chemical phenomena to material science has been addressing by the scientific society at the nanoscale [11]. Nanoparticle doping technology provides a more convenient and flexible approach for the modification of liquid crystal materials and for designing new and improved devices based upon LCs. Moreover, different nanoparticle dispersion in Liquid crystals has enhanced the physical properties of LCs. LCs act as tunable solvents for the dispersion of nanomaterials and LCs being anisotropic media, they provide a very good support for the self assembly of nanomaterials in to large organized structures in multiple dimensions. Hence LC mediated self assembly can be efficiently used to organize different kinds of nanomaterials in to soft and well defined functional super structures. Zinc oxide (ZnO) nanoparticles have become famous among researchers due to its use in various applications like gas sensors [12], chemical sensors [13], biosensors [14], superconductors [15], photocatalyst [16], optoelectronic devices [17], cosmetics etc. ZnO is a wide band gap semiconductor having high optical transparency and luminescence in visible and near ultraviolet range of spectrum. Therefore, it is usually used in light emitting diodes and solar cells. Moreover Zinc Oxide is environmental friendly and ease to synthesize. Rao et al. have presented the results on different oxide materials in their earlier studies [18-30].

EXPERIMENTAL

Synthesis of ZnO Nanoparticles–High Pressure Combustion Synthesis (High Pressure Autoclave)

Take a known amount (3 g) of ZnO dissolved in 10 ml of conc. HNO_3 solution and 10 ml H_2O in 100 ml RB flask. The solution is stirred at ambient temperature for 1 hour. Then add Urea (reducing agent/fuel) which decomposes macro-molecules into nanoparticles. Now add 10 mol % flux (Boric Acid) and stirred the solution for 0.5 hour. Later keep the entire solutions into high pressure reactor at 120-130 ^oC maintaining a pressure of 200 Kg/cm^2 for 30 min. At this stage urea decomposes the entire solution in to ZnO nanoparticles. Then wash the resultant powder with methanol/ water 5 to 10 times and dried and finally ZnO nanoparticles of size nearly 70 nm are obtained. These nanoparticles are further characterized by UV-Visible Spectroscopy and SEM experimental techniques.

Dispersion of Nanoparticles into the LC compounds

For uniform dispersion of nanoparticles in LCs, the nanoparticles are first dissolved in ethyl alcohol, stirred well about 45 minutes and later introduced in the isotropic state of mesogenic material (8OBA & 12OBA) in quantity 0.5 wt % separately. After cooling, the nanocomposite 8OBA & 12OBA is subjected to study of the textural and phase transition temperatures using a polarizing optical microscope (SDTECHS make) with a hot stage in which the substance was filled in planar arrangement in 4 μm cells and these could be placed along with the thermometer described by Gray [31]. Textural and phase transition temperatures are studied after preparation of the sample and observations are made again to understand the stability of nanoparticles. The presence of citrate capped Au nanoparticles in 8OBA & 12OBA is studied by UV and SEM data and existence as well as size is determined by XRD technique.

Periodic Noise Reduction Using Frequency Domain Filtering

When equipment similar to the equipment that generated a degraded image is available, it is generally possible to determine the nature of the degradation by experimenting with various equipment settings. However, relevant imaging equipment availability is the exception, rather than the rule, in the solution of image restoration problems, and a typical approach is to experiment by generating PSFs and testing the results with various restoration algorithms. Finally, when no information is available about the PSF, we can resort to “blind de-convolution” for inferring the PSF. One of the principle degradations encountered in image restoration problems is image blur. Blur that occurs with the scene and sensor at rest with respect to each other can be modeled by frequency domain low pass filters. Another important degradation model is image

ISSN: 0975-8585

blur caused by uniform linear motion between the sensor and scene during image acquisition. Periodic noise produces impulse-like bursts that often are visible in the Fourier spectrum. The principal approach for filtering these components is to use notch reject filtering. The general expression for a notch reject filter having Q notch pairs is

$$H_{NR}(u, v) = \prod_{k=1}^{Q} H_k(u, v) H_{-k(u,v)}$$

Where $H_k(u, v)$ and $H_{-k}(u, v)$ are high pass filters with centers at (u_k, v_k) and $(-u_k, -v_k)$, respectively. These translated centers are specified with respect to the center of the frequency rectangle, (M/2, N/2). Therefore, the distance computations for the filters are given by the expression

$$D_k(u, v) = [(u-M/2-u_k)^2 + (v-N/2-v_k)^2]^{1/2}$$

and

$$D_{-k}(u, v) = [(u-M/2+u_k)^2 + (v-N/2+v_k)^2]^{1/2}$$

A special case of notch rejects filtering that notch out components along of the frequency axes also are used for image restoration.

RESULTS AND DISCUSSION

Polarizing Optical Microscope

Determination and characterization of these mesophases will provide very important information on the pattern and textures of the liquid crystals. The transition temperatures and textures observed by Polarizing Microscope in 8OBA pure is shown in Figure-1(a-d) while that of with dispersed ZnO nanoparticles with concentration 0.5 wt % shown in Figure-2(a-d) respectively. The thermal range of nematic phase is changed slightly due to the dispersion of nanoparticles and the textures of the phase's changes by the self assembly of nanoparticles. The DSC thermograms are shown in Figure-3 to Figure-6. The transition temperatures at the phase transformations determined through POM is shown in the Table-1. The compound 8OBA and 12OBA are brought from sigma-Aldrich, USA and used as such. For uniform dispersion of ZnO nanoparticles in 8OBA and 12OBA, the nanoparticles are first dissolved in ethyl alcohol, stirred well about 45 minutes and later introduced in the isotropic state of mesogenic material in the ratio of 0.5 wt % concentration separately.

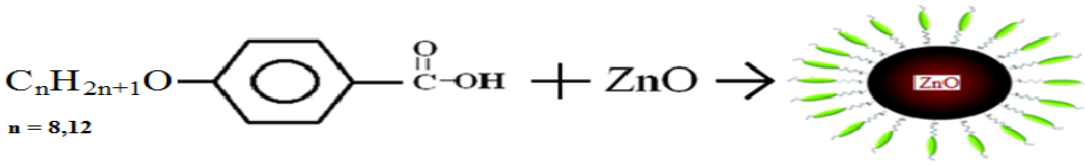

Table 1: Phase variants, Transition temperatures, Enthalpy values of 8OBA and 12OBA pure and with dispersed 0.5 wt% ZnO nanoparticles

S. No	Compound	DSC/ POM	Scan Rate	Transition Temperatures °C				Thermal Ranges	
				I-N	N-SmC	SmC-Solid I	SolidI – Solid II	ΔN	ΔSmC
1	8OBA PURE	DSC	20c/min ΔHJ/gm	144.2 3.16	105.56 3.42	95.5 22.77		38.64	10.06
		POM		143.92	104.9	95.2		39.02	9.7

ISSN: 0975-8585

2	8OBA + 0.5 wt % ZnO	DSC	20C/min ΔHJ/gm	143.15 5.96	104.37 3.10	93.73 28.12		38.78	10.64
		POM		143.4	103.7	95.2	89.2	39.7	8.5
3	12OBA PURE	DSC	20c/min ΔHJ/g	138.8 1.49	132.8 7.91	97.3 81.03		6	35.5
		POM		138.1	130.4	96.4		7	34
4	12OBA + 0.5 wt % ZnO	DSC	20c/min ΔHJ/g	129.22	120.9	86.39	65.33	8.3	34.51
		POM		127.7	119.8	91.2	79.0	7.9	28.6

Figure-1(a-d): POM Textures of 8OBA + 0.5 wt% ZnO

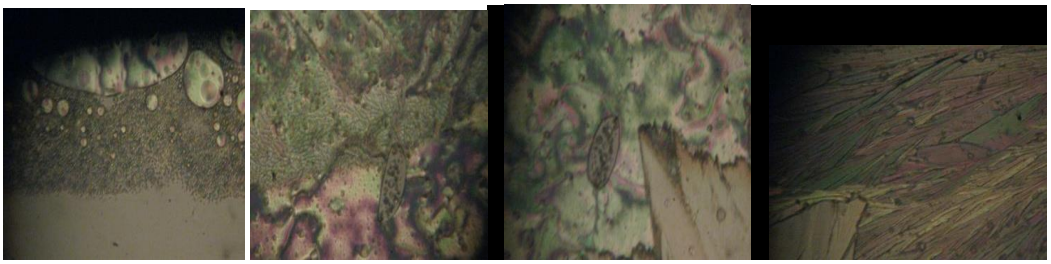

(a) Nematic phase at 143.4 ^{O}C | (b) Nematic-Smectic C at 89.2 ^{O}C | (c) Solid I at 103.7 ^{O}C | (d) Solid I at 95.2 ^{O}C

Figure-2(a-d): POM Textures of 12OBA + 0.5 wt% ZnO

(a) Nematic phase at 145.2 ^{O}C | (b) Nematic -Smectic C at 77.5 ^{O}C | (c) Solid I at 136.6^{O}C | (d) Solid I at 92.6^{O}C

Figure-3: DSC thermogram of 8OBA Pure

ISSN: 0975-8585

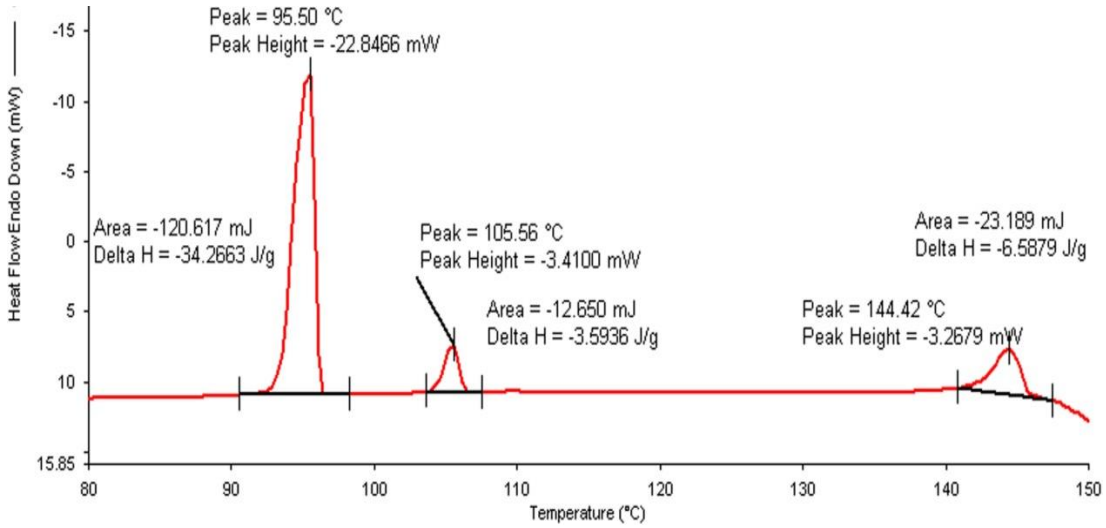

Figure-4: DSC thermogram of 12OBA Pure

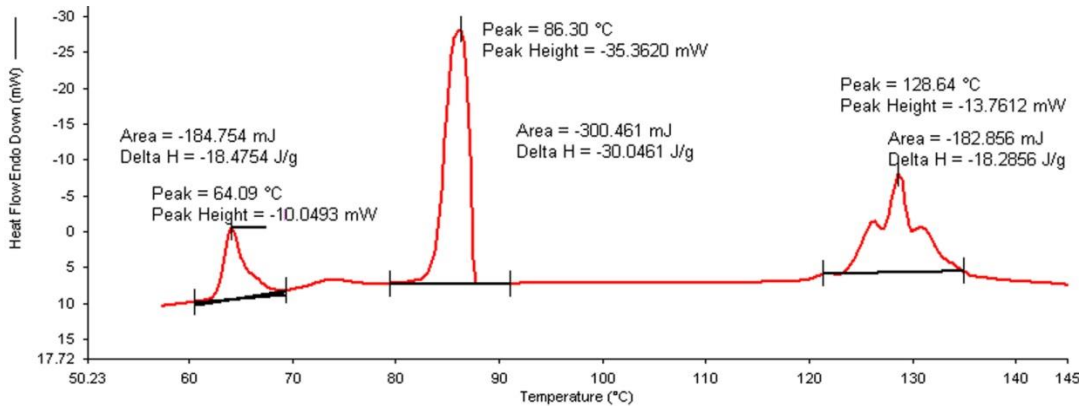

Figure-5: DSC thermogram of 8OBA with 0.5 wt % ZnO nanoparticles

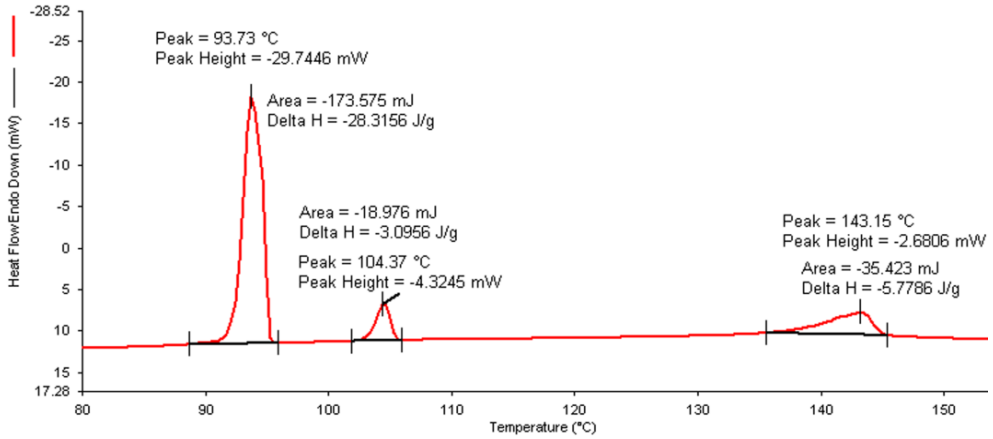

Figure-6: DSC thermogram of 12OBA with 0.5 wt % ZnO nanoparticles

ISSN: 0975-8585

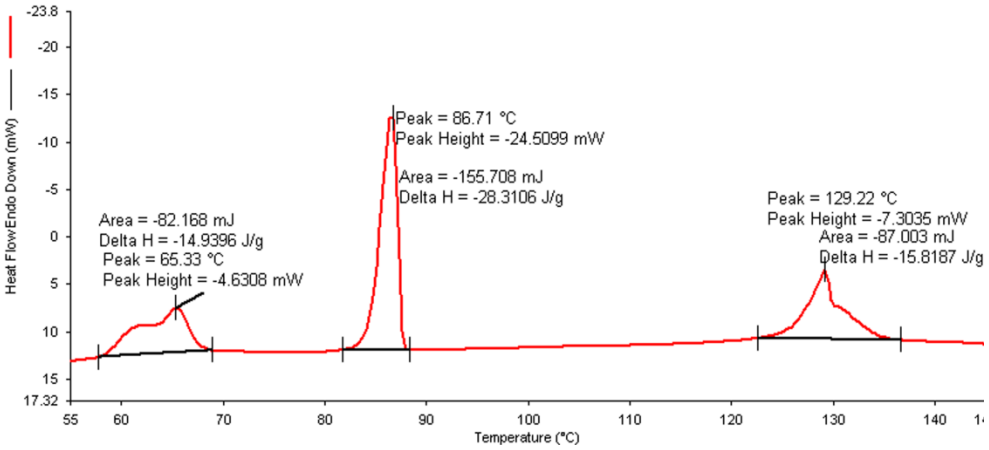

FTIR Analysis

As synthesized ZnO nanoparticles dispersed in 12OBA Compound is analyzed by using FTIR at room temperature. The compound is stable at room temperature, the IR frequencies in solid state which are correlated in bond with the pure bond 12OBA. The assigned bonds corresponding to the resultant frequencies from the spectra are tabulated. Due to the excitation of both molecular vibrations and rotations absorptions of electromagnetic radiation causes the formation of absorption bands in the IR spectra which are useful to explain the bonding interaction of the molecules. In both spectra exhibit a strong electromagnetic absorption at 1609.97 cm^{-1}, 1599.63 cm^{-1} and 1256.26 cm^{-1}, 1256.26 cm^{-1} corresponding to aromatic ring stretching. The absorption bands at 2915.53 cm^{-1} and 2918.77cm^{-1} are corresponding to OH bond. The existence of OH bond vibration at 647.77 cm^{-1}, 654.24 cm^{-1} and also represents the benzoic acids moiety due to their strong intensity and strongly supports the existence of 12OBA. The bond 843.70 cm^{-1}, 843.70 cm^{-1} are assigned to stretching ring vibration at the out of plane. While dispersing the ZnO nanoparticles the intensity of the peaks are found to be decreased as shown in the Figure-7 and Table-2. The intensity of 12OBAwith dispersed nanoparticles is found be decreases, this related to the change in dipole that occurs during the vibration. The vibrations that produce small change in dipole result in a less intense absorption than those that result in a relatively modest change in dipole. As we have taken the FTIR data in mid infra red region, it is not possible to take the nanoparticle data.

Figure-7: FTIR of 12OBA pure and with dispersed 0.5 wt % ZnO nanoparticles

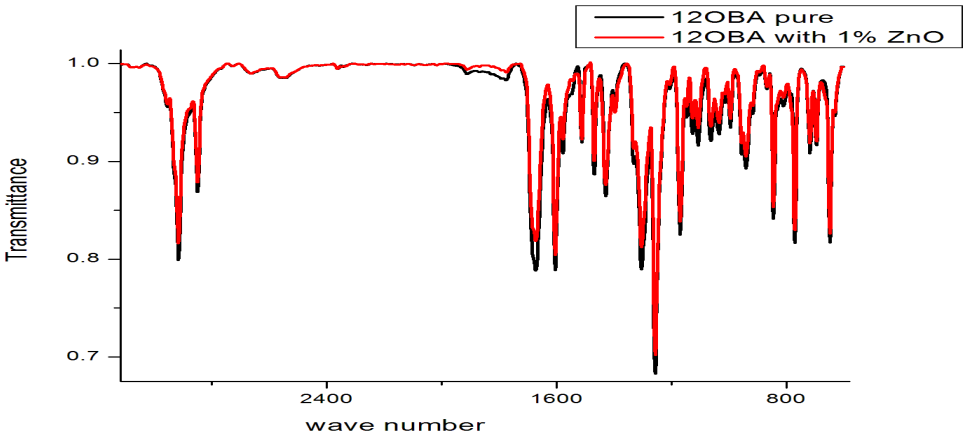

ISSN: 0975-8585

Table-2: Functional group intensities for 12OBA pure and with dispersed ZnO nanoparticles across the following wavelengths

S.No.	Wavenumer cm^{-1}	Intensity for pure LC	Intensity for LC with dispersed ZnO nanoparticles	Functional Group
1	2915.53	0.8040	0.8389	OH bond
2	1669.46	0.78778	0.8235	Benzoic acid
3	1609.97	0.7938	0.8167	Ring stretching
4	1575.05	0.9094	0.9212	
5	1508.45	0.9153	0.9339	
6	1469.65	0.8856	0.9103	
7	1298.29	0.7981	0.8210	dimer
8	1256.26	0.6885	0.7216	Aromatic ring structure
9	1168.96	0.8261	0.8499	CHOH bending
10	843.7	0.8397	0.8686	Ring out of plane pplane
11	766.75	0.8159	0.8686	Aromatic ring stretching
12	720.84	0.9086	0.9221	CH out of plane
13	693.39	0.9136	0.9280	C=O bending
14	647.77	0.8184	0.8380	OH bond

UV-Visible Analysis

The UV-Visible analysis of 12OBA with 0.5 wt % ZnO nanoparticles is shown in Figure-8. The peaks between 245 to 258 nm resemble the existence of ZnO nanoparticles in the LC compound. So, the UV-visible spectral study confirms the presence of Zno nanoparticles in the prepared nanodoped LC.

Figure-8: UV Analysis of 12OBA with dispersed 0.5 wt % ZnO nanoparticles

ISSN: 0975-8585

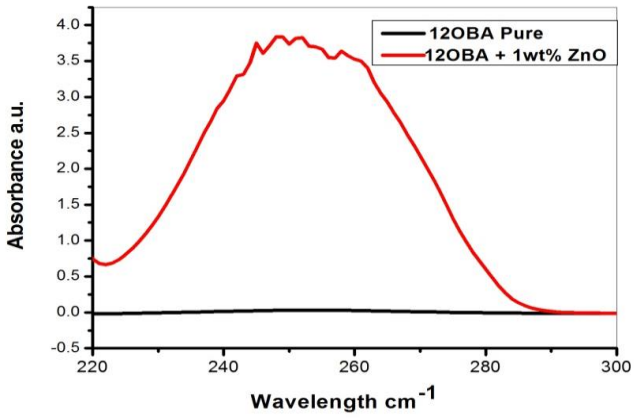

SEM Analysis

SEM gives the magnified image of the surface of a material, topographical information and also gives the information regarding the composition of the elements in the material (Figure-9 and Figure-11). The SEM images of ZnO nanoparticles and with the dispersion of 1 wt % ZnO nanoparticle in 12OBA is shown in the Figure-10 and Figure-12.

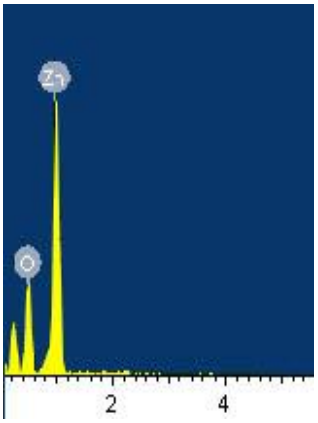

Figure-9: EDS data of ZnO nanoparticles

Element	Weight%	Atomic%
O K	26.28	59.29
Zn L	73.72	40.71

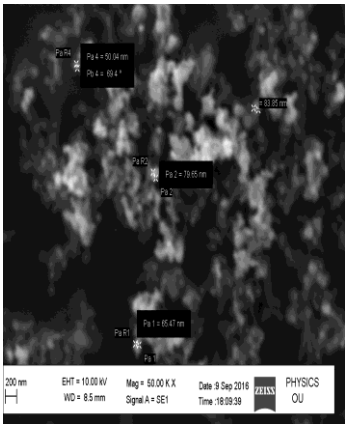

Figure-10: SEM Image

ISSN: 0975-8585

Element	Weight%	Atomic%
C K	80.29	85.23
O K	18.15	14.46
Zn L	1.57	0.31

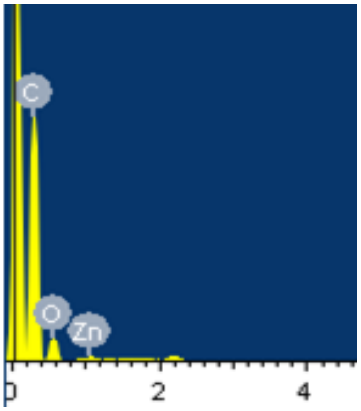

Figure-11: EDS data of 12OBA with Image dispersed ZnO nanoparticles

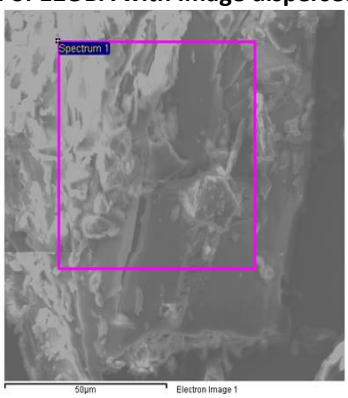

Figure-12: SEM Image

Frequency domain filtering analysis in Image processing

The nanodispersed liquid crystal compound images collected from POM and observed that the images quality is very poor with respect to contrast. Frequency domain filtering technique is applied to enhance the images and the corresponding enhanced images are presented in this section (Figure-13(a-d) to Figure-16 (a-d)).

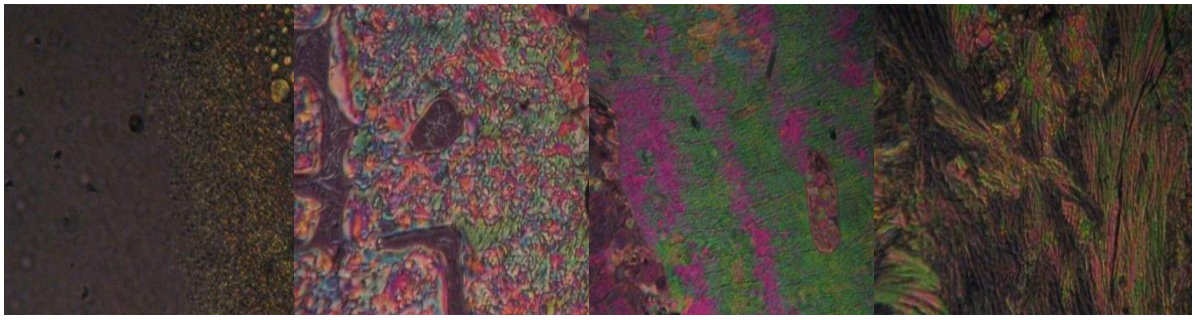

(a) Nematic phase at 145.2 ^{O}C | (b) Nematic-Smectic C at 136.6 ^{O}C | (c) Solid I at 92.6 ^{O}C | (d) Solid I at 77.5 ^{O}C

Figure-13(a-d): Texture of 12OBA + 0.5 wt% ZnO (POM Images)

ISSN: 0975-8585

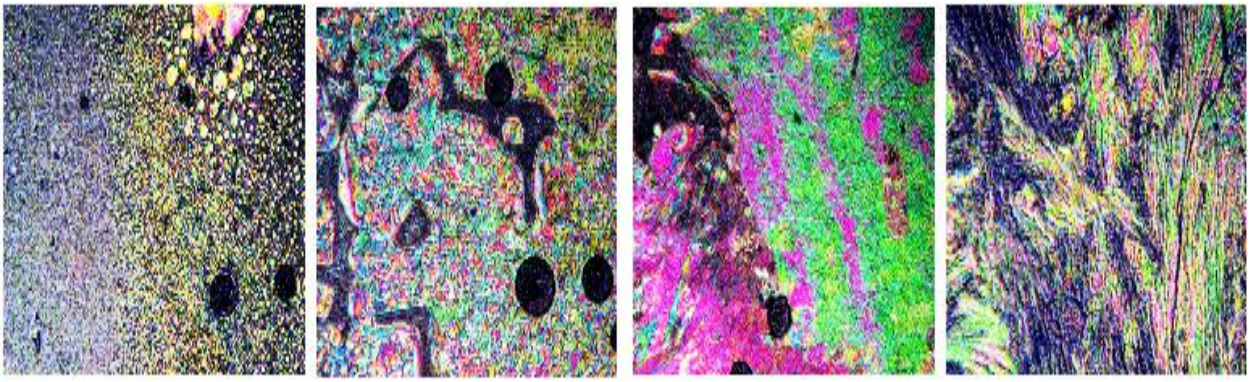

Figure-14(a-d): Contrast enhanced Images of 12OBA + 0.5 wt % ZnO using Image Processing)

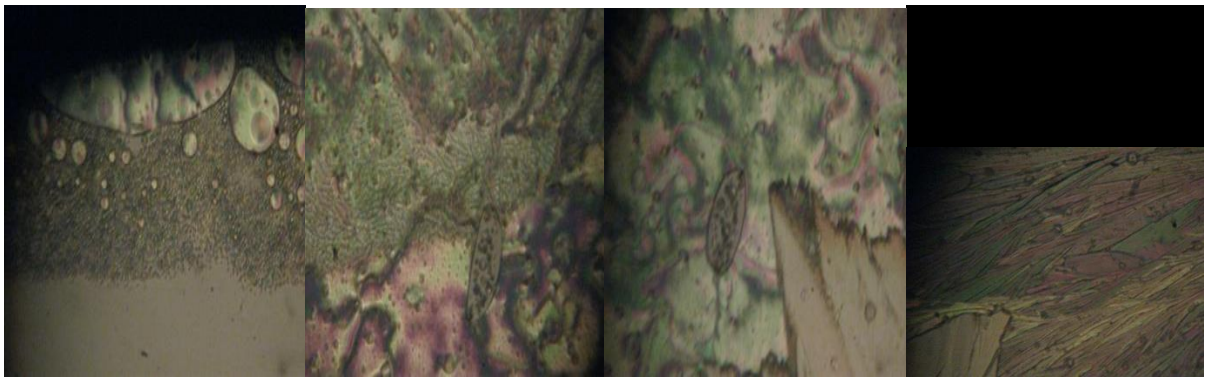

(a) Nematic phase at 143.4 ^{O}C | (b) Nematic-Smectic C at 103.7 ^{O}C | (c) Solid I at 95.2 ^{O}C | (d) Solid I at 89.2 ^{O}C

Figure-15(a-d): Texture of 8OBA + 0.5 wt% ZnO (POM Images)

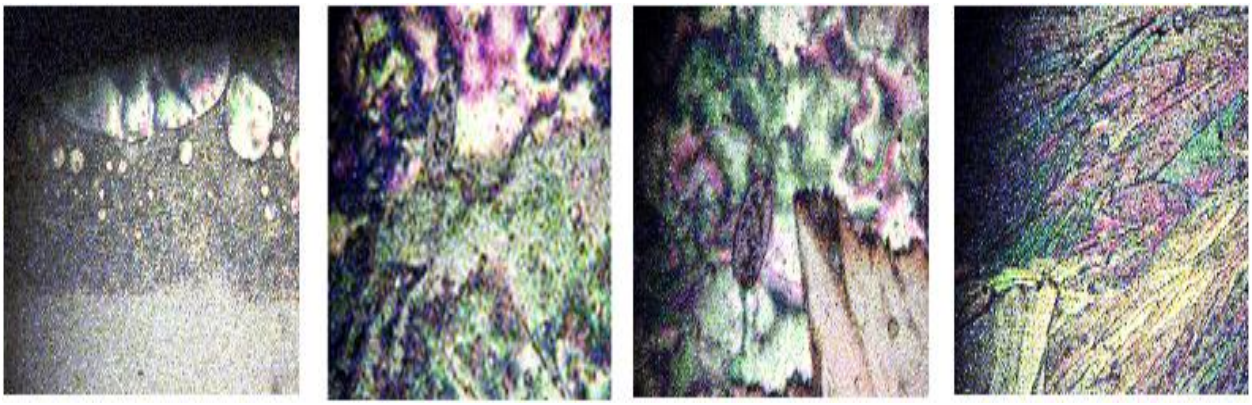

Figure-16(a-d): Contrast enhanced Images of 8OBA + 0.5 wt % ZnO using Image Processing

CONCLUSIONS

With the present results we demonstrated the dispersion of ZnO nanoparticles in LC 8OBA and 12OBA changing of their textures, phase transition temperatures and shifts in vibrational bands by using Polarizing Microscope, Differential Scanning Calorimeter and Fourier Transform Infra Red techniques respectively. The transition temperatures obtained from polarizing microscope are in good agreement with those obtained from DSC. The UV-Visible spectral study confirms the presence of ZnO nanoparticles in the prepared nanodoped LC. The presence of ZnO in LC 12OBA is also confirmed by the EDS data of SEM and the ZnO nanopartilces sizes are

in the range of 50-85 nm. To enhance the image quality, frequency domain filtering technique in image processing is used and the enhanced images are giving better contrast to identify the transition phases.

ACKNOWLEDGEMENTS

The Corresponding author Dr R.K.N.R. Manepalli (Dr M. Ramakrishna Nanchara Rao) is thankful to the UGC for grant 42-784/2013 (SR).

REFERENCES

[1] Kato T, Mizoshita N, Kishimoto K. Angew Chem Int Ed 2006; 45: 38-68.
[2] Goodby JW, Saez IM, Cowling SJ, Gortz V, Drapper M, Hall AW, Sia S, Cosquer G, Lee SE, Raynes EP. Angew Chem Int E 2008; 47: 2754-2787.
[3] Tschiersle C. Chem Soc Rev 2007; 36: 1930-1970.
[4] Shiraishi Y, Toshima N, Maeda K, Yoshikawa H, Xu J, Kobayashi S. Appl Phys Lett 2002; 81: 2845-2852.
[5] Lynch MD, Patrick DL. Nano Lett 2002; 2: 1197-1201.
[6] Dierking I, Scalia G, Morales PJ. J Appl Phys 2005; 97: 044309-1.
[7] Basu R, Iannacchione G. Appl Phys Lett 2008; 93: 183105-1.
[8] Lagerwall JPF, Scalia G. J Mater Chem 2008; 18: 2890-2898.
[9] Russell JM, Oh S, LaRue I, Zhou O, Samulski ET. Thin Solid Films 2006; 509: 53-57.
[10] Basu R, Iannacchione G. Phys Rev E 2009; 106: 124312-1.
[11] De Jong WH, Borm PJA. Int J Nanomedicine 2008; 3: 133-149.
[12] Gupta SK, Aditee Joshi, Manmeet Kaur. J Chem Sci 2010; 122: 57-62.
[13] Fan Z, Lu JG. IEEE Trans Nanotech 2006; 5: 393-396.
[14] Zhao Z, Lei W, Zhang X, Wang B, Jian H. Sensors 2010; 10: 1216-1231.
[15] Sharma P, Gupta A, Rao KV, Owens FJ, Sharma R, Ahuja R, Guillen JMO, Johnson B, Gehring GA. Nature Mater 2003; 2: 673-677.
[16] Bagabas A, Mohmed A, Aboud FA, Kosslick H. Nanoscale Res Lett 2013; 8: 516-526.
[17] Shao S, Zheng K, Zidek K, Chabera P, Pullerits T, Zhang F. Solar Ener Mater Solar Cells 2013; 118: 43-47.
[18] Rao MC. Optoelect & Adv Mater (Rapid Commu) 2011; 5(5-6): 651-654.
[19] Sivasri J, Rao MC, Giridhar G, Madhav BTP, Divakar TE, Manepalli R KNR, Rasayan J Chem 2016; 9(4): 556
[20] Jayaprada P, Tejaswi M, Giridhar G, Rao MC, Pisipati VGKM, Manepalli RKNR, Rasayan J Chem 2016; 9(4): 588
[21] Tejaswi M, Rao MC, Datta Prasad PV, Giridhar G, Pisipti VGKM, Manepall RKNR, Rasayan J Chem 2016; 9(4): 697
[22] Rao MC, Ramachandra Rao K. Int J Chem Tech Res 2014; 6(7): 3931-3934.
[23] Rao MC. Int J Chem Tech Res 2014; 6(3): 1904-1906.
[24] Prasad PV, Ramachandra Rao K, Rao MC Int J Chem Tech Res 2014; 7(1): 269-274.
[25] Rao MC. Optoelect & Adv Mater (Rapid Commu) 2011; 5: 85-88.
[26] Muntaz Begum Sk, Rao MC, Ravikumar RVSSN. Spectrochim Acta Part A Mol & BiomolSpec 2012; 98: 100-104.
[27] Muntaz Begum Sk, Rao MC, Ravikumar RVSSN. J Inorg Organometa Poly Mater 2013; 23(2): 350-356.
[28] Rao MC. J Optoelect & Adv Mater 2011; 13: 428-431.
[29] Rao MC, Hussain OM. Eur Phys J Appl Phys 2009; 48(2): 20503
[30] Ravindranadh K, Rao MC, Ravikumar RVSSN. J Luminesce 2015; 159: 119-127.
[31] Gray GW. Molecular structures and properties of liquid crystals, Academic press, 1962.